Supplemental Material

MATERIALS AND METHODS

Animal models

The *mkk4-flox* mice (referred to as $MKK4^{f/f}$) were previously generated (1). $MKK4^{f/f}$ mice were mated with mice expressing Cre under the myosin light chain (MLC2v) promoter to produce cardiomyocyte-specific MKK4 deletion ($MKK4^{cko}$) mice. $MKK4^{f/f}$ and $MKK4^{cko}$ mice were previously used for study the role of MKK4 in the development of cardiac hypertrophy (2). In the present study, $MKK4^{cko}$ and their littermate $MKK4^{f/f}$ mice were used to investigate the effect of MKK4 deficiency on ventricular arrhythmic susceptibility. The MLC2v-Cre line (kindly provided by Dr. KR Chien, Massachusetts General Hospital, USA) is a well established model that provides efficient ventricular-specific Cre recombinase expression and is known not to cause any abnormality in cardiac morphology and function following cardiac stress (3). All mice used in this study were maintained in a pathogen-free facility at the University of Manchester. The animal studies were performed in accordance with the UK Home Office and institutional guidelines.

Electrocardiography (ECG)

8-10 week old male $MKK4^{f/f}$ and $MKK4^{cko}$ mice were subjected to either sham or TAC operation for one week as previously described (2). To monitor cardiac rhythms at baseline and in hypertrophic condition we carried out *in vivo* ECG analysis (Power Lab/4SP with ML135 Dual Bio) on anesthetized mice. RR interval, P wave duration, PR interval, QRS and QT durations were recorded.

Programmed electrical stimulation (PES)

To assess propensity to ventricular arrhythmias, one week TAC-treated mice were anesthetized with Avertin (Sigma, 200 mg/kg), thereafter, an ultra miniature catheter (EPR-800, Millar Instruments) was inserted through the diaphragm directly arriving at the epicardial surface of the heart. PES was performed with a triggered stimulus isolation unit (DS2A, Digitimer) with the output set at 1.5 x diastolic capture threshold. The signals were amplified, filtered and digitized using an analogue-to-digital converter (CED 1401plus, Cambridge Electronic Design). A pacing train of eight stimuli (S1) was delivered at a basic cycle length of 100 ms, with a single (S2) premature extrastimulus introduced at progressively shorter intervals until an arrhythmia was induced or the ventricular refractory period was reached.

Epicardial activation mapping

Epicardial activation mapping of left ventricular free wall (LVFW) were recorded in isolated Langendorff-perfused hearts using a custom-made 64 separated electrodes (8 x 8 grids, 0.55 mm spacing). The total dimensions of the entire array are approximately 4 x 4 mm. The 64 recording electrodes were connected to two 32-channel amplifiers (SCXI-1102C, National Instruments Corporation Ltd, UK). The sampling frequency for each channel was set at 3 kHz. The signals were continuously recorded using a custom-developed program (Labview 7.1). The electrode terminals were positioned against the epicardial surface of the left ventricular free wall. To determine spread of electrical activation during basic stimulation, the epicardium was stimulated from two adjacent central electrodes in the grid at a basic cycle-length of 100 ms. Propagation maps were then derived by off-line analysis. The signals were displayed on screen in sets of 8 to 16 electrograms. The activation time was determined as the point of maximal negative slope and marked with a cursor. After marking all significant waveforms in all leads, the activation times were then displayed in a grid representing the layout of the original recording array. All activation times were related to the timing of the first detected waveform. Isochrones were drawn manually around areas activated in steps of 1 ms. Conduction velocities were calculated from epicardial activation maps as previously described (4).

Mathematical modeling

A recent mathematical model for the electrical action potential (AP) of a single mouse ventricle myocyte by Bondarenko et al. (5) was used in this study. The model produces a ventricular APD_{90} of 20.5 ms. In order to study the effects of heterogeneous remodeling of Cx43 (i.e., gap junctional coupling) on the conduction velocity (CV) of ventricular excitation waves, the single cell model was incorporated into a diffusive reaction-diffusion partial differential equation (PDE) for multi-cellular ventricular tissue, which takes the form:

$$\frac{\partial V_m}{\partial t} = \nabla D(x, y)\nabla V_m + I_{ion} + I_{stim}$$

where $D(x, y)$ is the gap junctional coupling conductance with a base value of 0.011 mm^2/ms to give a solitary wave CV of 0.603 mm/ms, V_m is the membrane potential, I_{ion} is the membrane current, I_{stim} is the stimulus current.

The rate dependence of CV of ventricular excitation waves was studied by using an 1D model of a homogeneous tissue strand that consists 100 myocytes at an inter-myocyte distance of 0.05 mm with D being set to 0.011 mm^2/ms. Propagating excitation waves were initiated by applying an external stimulus current I_{stim} (- 80 pA/pF) to 3 myocytes at one end for 0.5 ms. CV restitution (CVr) was computed by using the standard S1-S2 protocol (6). With the S1, 5 conditioning stimuli were applied with a pacing cycle length (PCL) at 100 ms, after the 5^{th} S1 stimulus, a premature stimulus (S2) was applied at progressively smaller time intervals. CVr curves were constructed by plotting the CV of the final propagating excitation against the S1-S2 interval (7). Wavelength was computed as the product of APD_{90} and solitary wave CV.

The effects of heterogeneous remodeling of Cx43 on CV were studied by using a 2D model of ventricular tissue with a size of 10 mm x 10 mm (consisting of 200 x 200 cells). In this method, randomly shaped "patches" of remodeled Cx43 were distributed in the 2D model. The size of the patch was taken to be less than half of wavelength of control wave. The amount of patches was progressively increased in simulations. Under this condition, planer wave (mimicking physiological propagations) and circular wave of excitation were considered.

Preparation of lysates and immunoblot analysis

Proteins were homogenized and extracted from NRCMs or tissues in RIPA lysis buffer (20 mM Tris-HCl, pH 7.4, 137 mM NaCl, 2 mM EDTA, 1% Triton X-100, 25 mM ß-glycerophosphate, 10% glycerol, 1 mM orthovanadate, 1 mM phenylsulphfonyl fluoride, 10 µg/ml leupeptin, 10 µg/ml aprotinin). Protein extracts (50 µg) were subjected to Western blot analysis with antibodies against Cx43, N-cadherin, β-catenin, plakoglobin, tubulin (Sigma); ZO-1 (Zymed); MKK7, c-Jun, phospho-cJun, JNK and phospho-JNK (Cell Signalling); MKK4 (BD Pharmingen). Immunecomplexes were detected by enhanced chemiluminescence with anti-mouse or anti-rabbit immunoglobulin G coupled to horseradish peroxidase as the secondary antibody (Amersham-Pharmacia).

Quantitative real-time PCR

Total RNA was prepared from NRCMs or ventricular tissues using Trizol reagent, followed by the synthesis of cDNA. Real-time quantitative PCRs were performed using the SYBR-green I Core Kit (Eurogentec). The primers used for detection of Cx43 and GAPDH expression were obtained from Qiagen. PCR products were detected in the ABI-PRISM 7700 sequence detection system (Applied Biosystems), and the results were analyzed using the $2^{-\Delta\Delta CT}$ method (8). The level of expression of Cx43 mRNA was normalized to that of GAPDH mRNA.

Immunohistochemical analyses

Fresh cryosections of ventricular tissues fixed in ice-cold acetone-methanol were used to analyze Cx43, N-cadherin, β-catenin and plakoglobin by indirect immunofluorescence. The sections were incubated with the following primary antibodies: Cx43, N-cadherin, β-catenin, plakoglobin (Sigma); ZO-1 (Zymed). As secondary antibodies, goat anti-mouse or goat anti-rabbit antibodies,

conjugated to Alexa Fluoro 488 (Invitrogen), or Alexa Fluoro 568 (Invitrogen), respectively, were used. The slides were viewed and analyzed using a Nikon Eclipse E600 microscope. To quantify fluorescence intensity and the number of Cx43-positive clusters, the settings of the fluorescence microscope were kept the same for all samples. For each animal, 20 randomly chosen fields of Cx43 antibody immunostained-sections were measured to quantify fluorescence intensities by the Image J analysis system and expressed as mean pixel density. The number of Cx43-positive clusters was quantified by counting the visible aggregates per unit area from 10 randomly chosen fields for each animal.

Transmission electron microscopy (TEM)

Heart samples were firstly fixed overnight in the fixative buffer (2.5% glutaraldehyde in 0.1 M sodium cacodylate solution containing 0.5 mM $CaCl_2$, pH 7.4), and then in 0.1 M sodium cacodylate solution containing 1% OsO_4 for a further 1h. After washing in distilled water, the samples were stained with 1% uranyl acetate at 4°C overnight. Subsequently, after being dehydrated in ethanol, the heart samples were embedded in TAAB resin and polymerized at 60°C for 72h. Ultrathin sections (50 nm) were obtained and examined on an FEI Technai 12 Biotwin electron microscope.

siRNA transfection

Primary cultures of neonatal rat cardiomyocytes (NRCMs) were prepared as previously described (2). NRCMs were transfected with siRNA (100nM) using Lipofectamine Plus reagent according to the manufacturer's instructions (Invitrogen). Rat MKK4 siRNA (gene ID # 287398; si genome SMART pool) was purchased from Dharmacon, siRNA negative control (Si Neg) was obtained from Eurogenetec.

Adenovirus vector construction

The rCx43 promoter region (-148, +281, containing two AP-1 binding sites) was previously cloned in the pGL3-Basic vector (9). Using this vector as a template, we created a single mutations at either the AP-1 (-47, -39) site, or the AP-1 (-122, -112) site, or double mutations at both AP-1 sites by QuikChange site-directed mutagenesis kit (Stratagene). All constructs were verified by DNA sequencing. Adenovirus expressing wild type Cx43 promoter-Luc (referred to as Ad-Cx43APwt-Luc), single mutation at the (-47, -39) site (referred to as Ad-Cx43APma-Luc), single mutation at the (-122, -112) site (referred to as Ad-Cx43APmb-Luc) and double mutations at two sites (referred to as Ad-Cx43APdm-Luc) were generated using ViraPower Adenoviral Expression System (Invitrogen). Adenovirus encoding GFP (Ad-GFP) was used as a control virus. Adenovirus encoding constitutively active MKK4 (Ad-caMKK4) was a kind gift from Dr. Hiroki Aoki (Kurume University, Japan); Adenovirus expressing the dominant-negative form of MKK4 (Ad-dnMKK4) was purchased from Seven Hills Bioreagents.

Luciferase reporter assay

48h post-transfection of siRNA, NRCMs were infected with Ad-Cx43APwt-Luc at 25 MOI in serum-free medium. At 24h after infection, the virus was removed. Following phenylephrine (PE) treatment (100 μM, 24h), aliquots of NRCM lysates were assayed for luciferase activity using a luciferase assay kit (Promega). To measure rCx43 promoter-luciferase activity after blocking MKK4 activation, cardiomyocytes were infected with Ad-dnMKK4 (25 MOI) for 24h prior to the infection of Ad-Cx43APwt-Luc (25 MOI) for a further 24h. After the removal of the viruses, cardiomyocytes were treated with 100 μM PE for 24h followed by the luciferase assay. To determine whether MKK4-regulated Cx43 transcription is dependent on AP-1 transcriptional activity, NRCMs were first infected with either Ad-GFP or Ad-caMKK4 at 25 MOI in serum-free medium. Following 24h of infection, Ad-Cx43APwt-Luc, or Ad-Cx43APma-Luc, or Ad-Cx43APmb-Luc, or Ad-Cx43APdm-Luc was added to either Ad-GPF-NRCMs or Ad-caMKK4 -NRCMs for a further 24h. Then, luciferase activity in each experimental group was measured described as above.

REFERENCES

1 Wang, X., Nadarajah, B., Robinson, A.C., McColl, B.W., Jin, J.W., Dajas-Bailador, F., Boot-Handford, R.P., and Tournier, C. (2007) *Mol. Cell. Biol.* **27,** 7935-7946

2 Liu, W., Zi, M., Jin, J.W., Prehar, S., Oceandy, D., Kimura, T.E., Lei, M., Neyses, L., Weston, A.H., Cartwright, E.J., and Wang, X. (2009) *Circ. Res.* **104,** 905-914

3 Minamisawa, S., Gu, Y., Ross, Jr J., Chien, K.R., and Chen, J. (1999) *J. Biol. Chem.* **274,** 10066-10070

4 Van Rijen, H.V.M., Eckardt, D., Degen, J., Theis, M., Ott, T., Willecke, K., Jongsma, H.J., Opthof, T., and de Bakker, J.M.T. (2004) *Circ. Res.* **109,** 1048-1055

5 Bondarenko, V.E., Szigeti, G.P., Bett, G.C.L., Kim, S.J., and Rasmusson, R.L. (2004) *Am. J. Physiol. Heart Circ. Physiol.* **287,** H1378–H1403

6 Kharche, S., Garratt, C.J., Boyett, M.R., Inada, S., Holden, A.V., Hancox, J.C., and Zhang, H. (2008) *Prog. Biophys. Mol. Biol.* **98(2-3),** 186-197

7 Kharche, S., Seemann, G., Margetts, L., Leng, J., Holden, A.V., and Zhang, H. (2008) *Concurrency Computat.: Pract. Exper.* **20,** 1317-128

8 Livak, K.L., and Schmittgen, T.D. (2001) *Methods* **25,** 402-408

9 Teunissen, B.E.J., Jansen, A.T., Van Amersfoorth, S.C.M., O'Brien, T.X., Jongsma, H.J., and Bierhuizen, M.F.A. (2003) *Gene* **322,** 123-136

LEGENDS

Supplemental Figure I. Analyses of junctional proteins by immunoblot analyses (A) and by immunohistochemstry (B) suggest that adherens junctions and desmosomes appear relatively normal in the $MKK4^{cko}$-TAC hearts. The ratios of N-cadherin/tubulin, β-catenin/tubulin and plakoglobin/tubulin are represented in the bar graphs in (A), n=6, data are mean ± SEM, n.s.: no difference found between two groups. Scale bar: 5 μm in (B).

Supplemental Figure II. Transmission Electron Microscopy of the $MKK4^{cko}$ heart. The overall cytoarchitecture of the $MKK4^{cko}$ cardiomyocyte appears normal and intact. The structure of myofibrils, sarcomere and Z-line in the mutants (II-IV) is comparable to the controls (I-III). Double-headed arrows show myofibrils and sarcomere, single-headed arrows point to Z-line in III-IV, scale bar: 500 nm. In V ($MKK4^{f/f}$) and VI ($MKK4^{cko}$), white arrow shows adherens junctions, and black arrow shows demosomal plaque, scale bar: 200 nm.

Supplemental Figure I

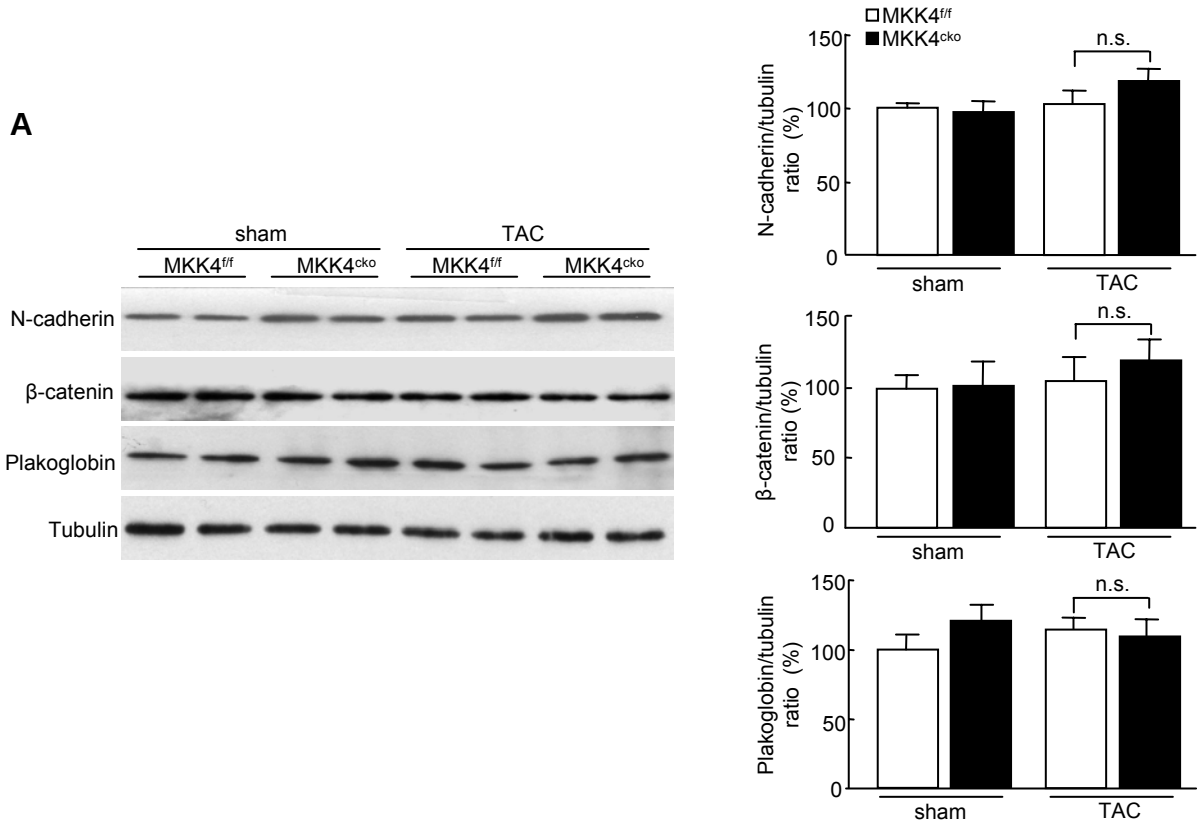

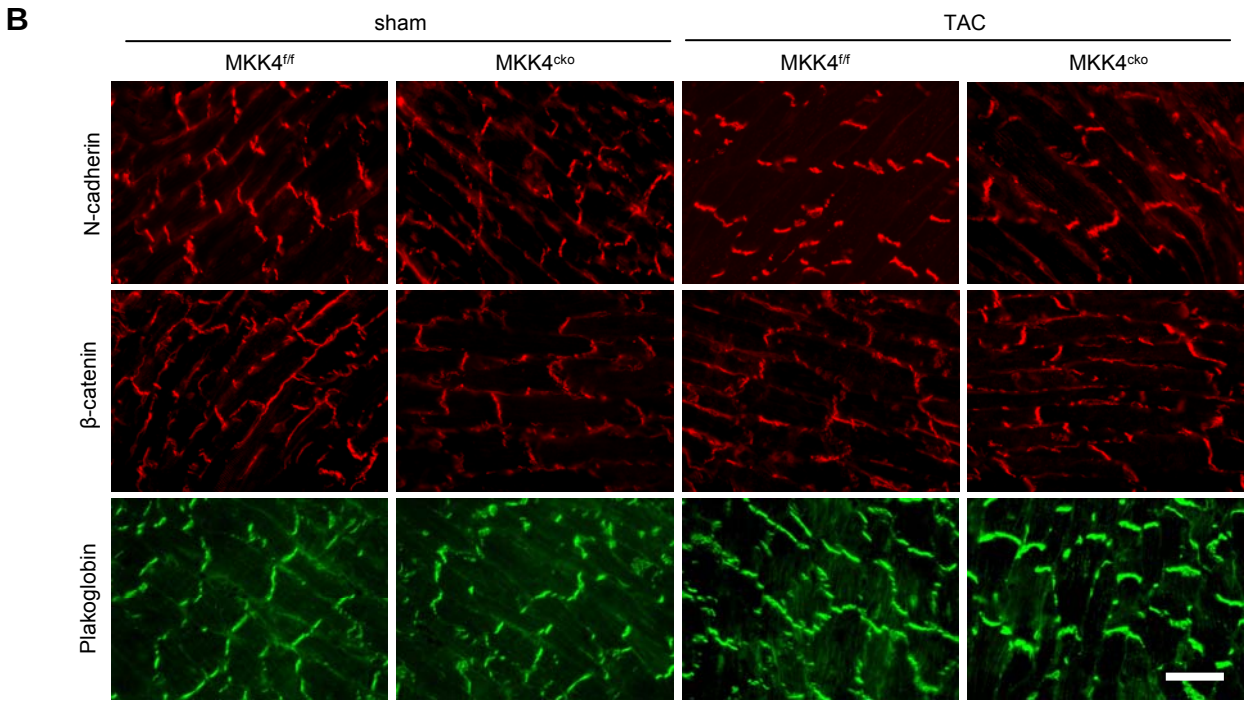

A